JACS
JOURNAL OF THE AMERICAN CHEMICAL SOCIETY

ARTICLE

pubs.acs.org/JACS

Structure and Lithium Transport Pathways in Li_2FeSiO_4 Cathodes for Lithium Batteries

A. Robert Armstrong,[†] Navaratnarajah Kuganathan,[‡] M. Saiful Islam,*[,‡] and Peter G. Bruce*[,†]

[†]School of Chemistry, University of St. Andrews, North Haugh, St. Andrews, Fife KY16 9ST, U.K.

[‡]Department of Chemistry, University of Bath, Bath, BA2 7AY, U.K.

Supporting Information

ABSTRACT: The importance of exploring new low-cost and safe cathodes for large-scale lithium batteries has led to increasing interest in Li_2FeSiO_4. The structure of Li_2FeSiO_4 undergoes significant change on cycling, from the as-prepared γ_s form to an inverse β_{II} polymorph; therefore it is important to establish the structure of the cycled material. In γ_s half the LiO_4, FeO_4, and SiO_4 tetrahedra point in opposite directions in an ordered manner and exhibit extensive edge sharing. Transformation to the inverse β_{II} polymorph on cycling involves inversion of half the SiO_4, FeO_4, and LiO_4 tetrahedra, such that they all now point in the same direction, eliminating edge sharing between cation sites and flattening the oxygen layers. As a result of the structural changes, Li^+ transport paths and corresponding Li−Li separations in the cycled structure are quite different from the as-prepared material, as revealed here by computer modeling, and involve distinct zigzag paths between both Li sites and through intervening unoccupied octahedral sites that share faces with the LiO_4 tetrahedra.

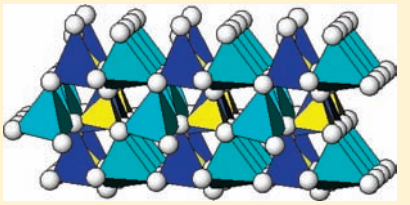

INTRODUCTION

There is intense interest in investigating Li intercalation compounds that might find application as cathodes in new generations of lithium-ion batteries. In this regard, one advantage of polyoxyanion intercalation compounds compared with transition metal oxides is that the binding of oxygen in the polyoxyanions enhances stability and thus safety. Phosphate cathodes, particularly $LiFePO_4$, have been extensively studied and continue to be important. The reason that silicates such as Li_2FeSiO_4 have attracted increasing attention recently is that iron and silicon are among the most abundant, and therefore lowest cost, elements on Earth. Developing cheap and safe cathode materials is a prime target for large-scale lithium batteries in the future.

Previous studies of Li_2FeSiO_4 have reported that more than 160 $mAhg^{-1}$ of charge can be extracted from Li_2FeSiO_4, with reversible capacities of 120−140 $mAhg^{-1}$.[1,2] Two other related Li intercalation hosts are known, Li_2MnSiO_4 and Li_2CoSiO_4.[3] The structure of as-prepared Li_2FeSiO_4 was reported recently.[4] However, it has been shown that the structure, and as a result the voltage, and polarization (and hence kinetics) of this cathode change during the first few cycles, then remain constant.[1b] Half of all the Li, Fe, and Si ions rearrange on cycling, which results in a significant change in the Li^+ diffusion pathways. Therefore, establishing the **cycled** structure of Li_2FeSiO_4 and its Li^+ diffusion pathways is important, to provide a platform on which future optimization of Li_2FeSiO_4 as a cathode for Li-ion batteries can be based. Here we report the crystal structure of cycled Li_2FeSiO_4 established using powder neutron diffraction and explore the Li^+ migration pathways using atomistic simulation techniques.

EXPERIMENTAL SECTION

Synthesizing phase pure Li_2FeSiO_4 has proved a challenge in the past; here we use the following method by Gong et al., which is known to produce a single phase material.[2d] Stoichiometric amounts of lithium acetate dihydrate (Acros), iron(II) acetate (Strem), and tetraethyl orthosilicate (Aldrich) were mixed in ethanol with 2 mL of acetic acid. After stirring, the suspension was transferred to a Teflon-lined autoclave and heated to 130 °C for 12 h. The resulting gel was dried under vacuum at 80 °C then mixed with sucrose and ball-milled under acetone for 30 min. Following acetone evaporation, the sample was annealed under flowing nitrogen at 600 °C for 10 h. All subsequent handling was carried out in an Ar-filled glovebox (oxygen and water levels <1 ppm). Powder X-ray diffraction data were collected on a Stoe STADI/P diffractometer operating in transmission mode with Fe $K\alpha_1$ radiation (λ = 1.936 Å) to eliminate Fe fluorescence.

Composite electrodes (Li_2FeSiO_4, super S carbon, and Kynar Flex 2801—a copolymer based on PVDF), with weight ratios 75:18:7, were constructed and incorporated into electrochemical cells with a lithium metal counter electrode and electrolyte (1 *m* LiTFSI in ethylene carbonate/diethyl carbonate 1:1). Electrochemical measurements were carried out at 50 °C using a Maccor Series 4200 battery cycler. After cycling, cells were opened in an Ar-filled glovebox, the active material removed and rinsed with dry solvent to remove residual electrolyte and binder, and dried. The samples were then transferred to 2 mm quartz capillaries for neutron diffraction measurements. Time-of-flight powder neutron diffraction data were obtained on the Polaris instrument at ISIS at the Rutherford Appleton Laboratory. Since lithium is a neutron absorber, the data for as-prepared materials were corrected for

Received: March 9, 2011
Published: July 08, 2011

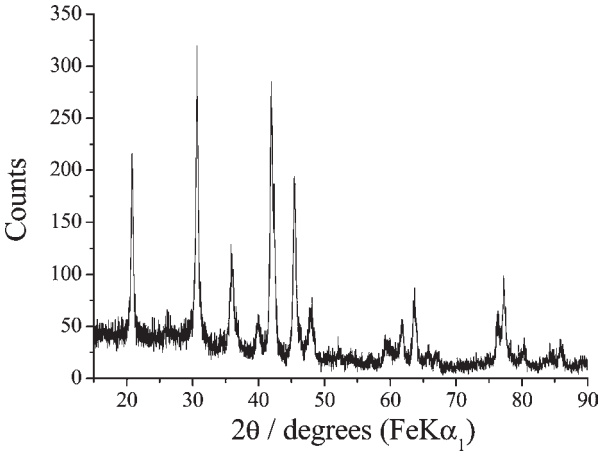

Figure 1. Powder X-ray diffraction pattern for as-prepared Li_2FeSiO_4.

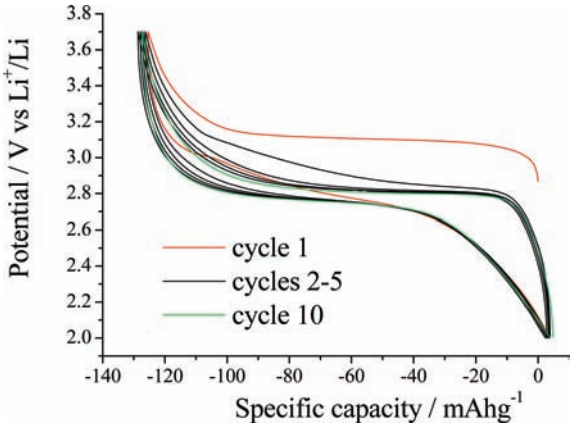

Figure 2. Variation of potential with state of charge on cycling Li_2FeSiO_4 at a rate of 10 mAg^{-1} (C/16) and demonstrating the change of potential and polarization upon cycling.

absorption. The structures were refined by the Rietveld method using the program TOPAS Academic.[5]

The atomistic modeling techniques are well-established and detailed elsewhere;[6] the interatomic interactions are treated by effective shell-model Buckingham potentials and a three-body term for the SiO_4 units (Table S2, Supporting Information). The transferability of this approach has proved successful in the modeling of structural, defect, and ion transport properties of Li_2MnSiO_4,[7] $LiFePO_4$,[8] and a range of apatite-silicates and zeolites.[6,9] An important feature of the methods is the treatment of full lattice relaxation of a large number of ions (>700) around the migrating lithium ion, which is modeled by the Mott–Littleton method (embodied in the GULP code).[6]

RESULTS AND DISCUSSION

The powder X-ray diffraction pattern of as-prepared Li_2FeSiO_4 is shown in Figure 1 and is in excellent agreement with previously reported data.[1,2,4] Electrochemical cells were constructed as described above and subjected to cycling; the load curve is shown in Figure 2. Consistent with previous reports, it exhibits a change of potential and a reduction in polarization (separation of charge and discharge curves) during the first few cycles, indicative of a change in structure, which nevertheless stabilizes after five cycles.[1,2] Mössbauer measurements indicate a small amount of Fe(III) (~10%) in this sample. We have

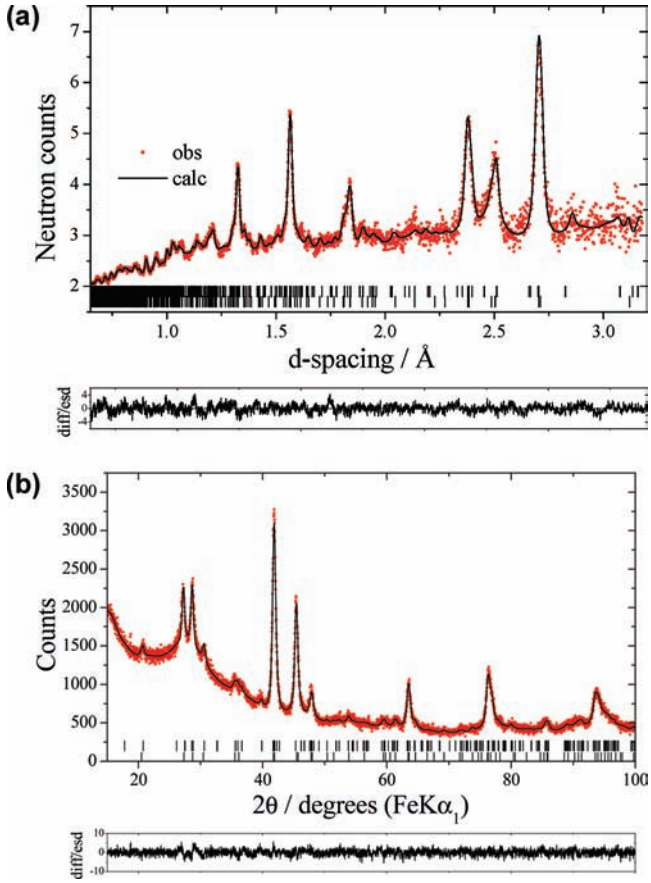

Figure 3. Fitted powder diffraction patterns for Li_2FeSiO_4 after 10 cycles at the end of discharge. (a) Neutrons. (b) X-rays. Dots represent observed data, and the solid line represents the calculated pattern. The lower line is the difference/esd. Tick marks indicate allowed reflections. Upper tick marks correspond to as-prepared Li_2FeSiO_4 (included as a second phase in the refinement) and lower tick marks to cycled structure.

prepared materials with up to 30% Fe(III) which exhibit phase transition behavior similar to that shown by the powder X-ray diffraction data in Figure S1 (Supporting Information).

Recent DFT calculations indicate that the change in structure on cycling leads to a drop in the cell voltage of ca. 0.3 V in good agreement with the observed change of potential (Figure 2) and is indicative of differences in the structure changing the site potential for lithium extraction.[10]

The structure of cycled Li_2FeSiO_4 was established using a combination of X-ray and neutron powder diffraction on material extracted from an electrochemical cell after 10 cycles. Li is a weak scatterer of X-rays but scatters neutrons relatively strongly, whereas Fe scatters both X-rays and neutrons strongly. Identifying the distribution of the Li ions in the structure is especially important as this information is used as the basis for modeling the Li^+ diffusion pathways, described later in the paper.

The fitted neutron and X-ray powder diffraction patterns for Li_2FeSiO_4 after 10 cycles at the end of discharge are shown in Figure 3. Li_2MSiO_4 compounds are known to exhibit complex polymorphism. Comparison of the powder diffraction data for cycled Li_2FeSiO_4 with data from other Li_2MSiO_4 phases suggested structural similarity with the β_{II} polymorph of Li_2CoSiO_4; therefore, this crystal structure was used as a starting point for

dx.doi.org/10.1021/ja2018543 |J. Am. Chem. Soc. 2011, 133, 13031–13035

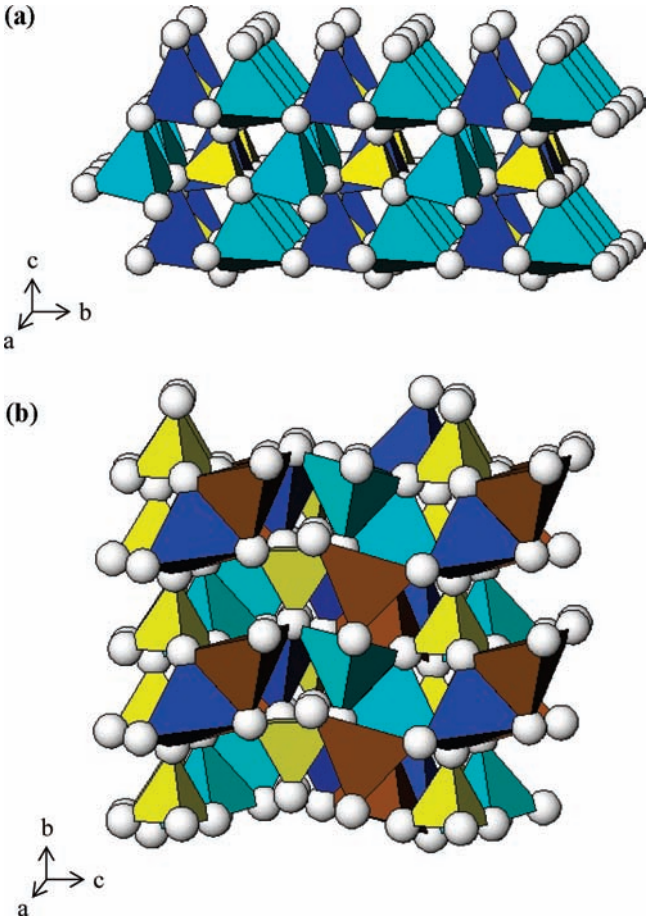

Figure 4. Crystal structures of (a) Li_2FeSiO_4 at the end of discharge after cycling, space group $Pmn2_1$. All tetrahedra point in the same direction along the *c*-axis and are linked only by corner-sharing; SiO_4 tetrahedra are isolated from each other, sharing corners with LiO_4 and $(Li/Fe)O_4$ tetrahedra. (SiO_4 tetrahedra, yellow; $Li1O_4$ tetrahedra, dark blue; $Li2/FeO_4$ tetrahedra, light blue). (b) As-prepared Li_2FeSiO_4, space group $P2_1/n$. In contrast to the β_{II}-type structure of the cycled material, the γ_s structure of as-prepared Li_2FeSiO_4 has half the tetrahedra pointing in opposite directions in an ordered fashion and exhibits edge sharing between pairs of LiO_4/FeO_4 and LiO_4/LiO_4 tetrahedra (SiO_4 tetrahedra, yellow; $Li1O_4$ tetrahedra, dark blue; $Li2O_4$ tetrahedra, light blue; FeO_4 tetrahedra, brown). The oxygen layers are also less buckled in the cycled material.

refinement of the cycled Li_2FeSiO_4 structure.[3d,11] An analogous model has also been suggested from DFT calculations.[12] A few small misfits were observed, which could be addressed by introducing the as-prepared structure as a minority second phase. In view of the complexity of the as-prepared structure, its atomic coordinates were fixed at the values obtained from refinement of the parent material (Table S1, Supporting Information) while allowing the lattice parameters to vary. The amount of this second phase refined to 10%. An excellent fit was obtained, R_{wp} of 2.6% (Figure 3). The particle size was extracted from the Rietveld refinement (peak widths), and a value of ~30 nm was observed, in good agreement with the particle size observed in TEM (Figure S2, Supporting Information). The final refined structure is shown in Figure 4 with coordinates in Table 1.

As for all Li_2MSiO_4 polymorphs, the O^{2-} ions adopt a distorted hexagonal close-packed arrangement, with half of the

Table 1. Refined Crystallographic Parameters for Li_2FeSiO_4 after 10 Cycles at the End of Discharge, Space Group $Pmn2_1$, and Result of Combined X-ray Neutron Refinement[a]

atom	Wyckoff symbol	*x*/*a*	*y*/*b*	*z*/*c*	B_{iso}
Li1	2a	0	0.147(7)	0.045(6)	0.7(-)
Si1	2a	0.5	0.175(2)	0	0.4(-)
Li2/Fe1[b]	4b	0.257(2)	0.342(2)	0.417(2)	0.4(2)
O1	4b	0.277(2)	0.332(2)	0.904(3)	1.7(2)
O2	2a	0	0.109(1)	0.396(3)	0.1(1)
O3	2a	0.5	0.157(2)	0.345(3)	0.1(1)

[a] R_e = 1.95%, R_{wp} = 2.61%, R_p = 2.67%, *a* = 6.236(3) Å, *b* = 5.423(2) Å, *c* = 4.988(2) Å. [b] Occupancy 0.49/0.51(2).

tetrahedral sites occupied by cations, such that face sharing is avoided. In the cycled structure, all the tetrahedra point in the same direction along the *c*-axis (Figure 4) and are linked only by corner-sharing. The SiO_4 tetrahedra are isolated from each other, sharing corners with LiO_4 and $(Li/Fe)O_4$ tetrahedra. In the ideal β_{II} structure, as adopted by Li_2MnSiO_4, the Li^+ and M^{2+} occupy different crystallographic sites. However, in cycled Li_2FeSiO_4, the site normally occupied by M^{2+} is occupied exclusively by Li^+, with the remaining Li^+ sharing the conventional Li site with the Fe ions; this structure is essentially the same as that adopted by the β_{II} polymorph of Li_2CoSiO_4 and is somewhat analogous to the relationship between normal and inverse spinels (Table 1).[13]

Previous powder X-ray data suggested that Li and Fe might both be distributed over two sets of sites, resulting in quite different pathways for Li migration from those reported here.[1b] The LiO_4 sites alternate with the SiO_4 tetrahedra along the *a*-axis, and the $(Li/Fe)O_4$ sites are also arranged in rows parallel to the *a*-axis (Figure 4). Refinement of the Li/Fe ratio on the shared site yielded a value of 0.49:0.51(2), implying an overall composition of $Li_{1.98}Fe_{1.02}SiO_4$, within 1 esd of the ideal stoichiometry. This is also in good agreement with the value obtained by counting charge on cycling (Figure 2). The load curves in Figure 2 were collected at a low rate of 10 $mAhg^{-1}$ and exhibit a plateau after ~5 cycles, suggesting intercalation may follow a two-phase process. Powder X-ray diffraction data at various states-of-charge after 5 cycles indicate strong structural similarity between the charged and discharged structures; however, attempts to refine a crystal structure for the charged cycled phase were unsuccessful, due in large part to the significant peak broadening, a process that is reversible on each cycle.

Comparing the structure of as-prepared and cycled Li_2FeSiO_4 indicates that significant structural change occurs within the first few cycles, emphasizing the importance of establishing the cycled structure (Figure 4). The structure of the former was refined using powder neutron diffraction data and gives an excellent fit (Figure S3, Table S1, Supporting Information) and agreement with the structure first reported by Yamada et al.[4] The space group used was $P2_1/n$, rather than the originally published $P2_1$.[14] The as-prepared structure, designated γ_s by Yamada, is shown in Figure 4. In γ_s, half the Li, Fe, and Si cations are in tetrahedral sites pointing along *c*, while the other half point in the opposite direction in an ordered manner; in contrast, in the cycled structure, all the Li, Fe, and Si cations are in tetrahedral sites pointing in the same direction along *c*. As a result of half the tetrahedra pointing in opposite directions, γ_s exhibits two sets of edge sharing tetrahedra: in the first set, each FeO_4 shares one edge with a LiO_4 tetrahedron, whereas in the second set two

Table 2. Calculated and Experimental Structural Parameters of the Cycled Li_2FeSiO_4 Material

parameter	calcd	exptl
a (Å)	6.3206	6.2361
b (Å)	5.4786	5.4231
c (Å)	4.8918	4.9881
$\alpha = \beta = \gamma$ (deg)	90.0	90.0
Li1−O (Å)	2.052	1.982
Li2−O (Å)	2.017	2.027
Fe−O (Å)	1.964	2.027
Si−O (Å)	1.635	1.688

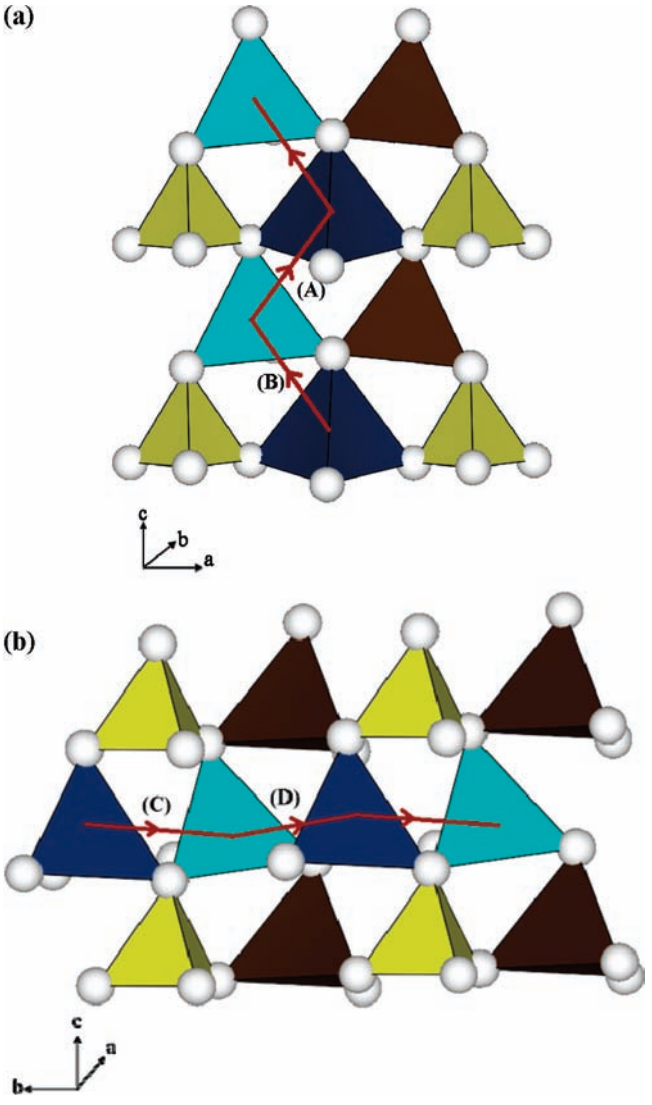

Figure 5. Pathways for lithium ion migration between corner-sharing Li(1) and Li(2) sites in the cycled structure of Li_2FeSiO_4. (a) The first path involves hops A and B in the c direction. (b) The second path involves hops C and D in the b direction (SiO_4 tetrahedra, yellow; Li(1)O_4 tetrahedra, dark blue; Li(2)O_4 tetrahedra, light blue; FeO_4 tetrahedra, brown).

LiO_4 tetrahedra share a common edge (Figure 4(b)); no edge sharing is observed in the cycled structure. The oxygen layers in the β_{II}-type cycled structure are significantly less buckled than in γ_s and more closely approach ideal hexagonal close packing. These differences in the structure on cycling change significantly the Li^+ diffusion pathways, something of considerable importance to the operation of the intercalation host as a cathode.

Table 3. Calculated Migration Energies and Interatomic Separations for Lithium-Ion Transport Paths in the Cycled Structure of Li_2FeSiO_4

migration path[a]	Li−Li separation (calcd) (Å)	E_{mig} (eV)
hops (A) + (B)	3.03 + 3.04	0.91
hops (C) + (D)	3.03 + 3.33	1.55

[a] Shown in Figure 5.

Before examining the diffusion pathways and activation energy for Li^+ ion transport, it was first necessary to consider how the Li/Fe ions that share a site might order. Diffraction data show no evidence for long-range order, so any order must extend over only limited distances. Different configurations of the shared (Li, Fe)O_4 sites were considered and included structures in which the LiO_4 and FeO_4 tetrahedra alternate regularly along the a-axis or align in parallel rows along the a-axis. The lattice energies of the various structures were then compared by performing a series of P1 geometry optimizations, allowing full relaxation of the ion positions and cell parameters. Our simulations find that the lowest-energy structure, by more than 110 meV, is the ordering scheme in which Li and Fe alternate regularly along the a-axis (Figure S4, Supporting Information).

Table 2 shows a comparison of the calculated and experimental structural parameters. The calculated unit cell parameters and Li−O, Fe−O, and Si−O bond lengths deviate from experiment by at most 0.09 Å and in most cases much less (e.g., Li2−O bonds); also, the observed unit cell volume is reproduced to within 0.4%. The minor discrepancies are possibly due to the calculated configuration of the shared (Li/Fe)O_4 site in the cycled structure. Nevertheless, the good reproduction of the relatively complex structure is not a trivial task and gives us confidence that the simulation model can be used reliably in the lithium migration calculations.

The lithium diffusion paths in the cycled (β_{II}) structure of Li_2FeSiO_4 have not been clearly established before. Previous DFT studies[15] based on earlier structural data have examined similar migration paths in the delithiated system. Our previous studies[7,8] have shown that simulation techniques can be used to examine defects and migration mechanisms, which are often difficult to probe by experiment.

For the cycled structure, we have identified two main Li migration paths illustrated in Figure 5, with the Li−Li hop distances listed in Table 3. The first path involves corner-sharing Li1 and Li2 sites with an overall trajectory along the c-axis direction; the second path also involves hops between Li1 and Li2 sites but in the b direction with longer hop distances. We note that the Li^+ transport paths and Li−Li hop distances in the cycled structure are quite different from the as-prepared material, in keeping with the significant structural reorganization; for example, our structural data for the as-prepared γ_s material (Table S1, Supporting Information) indicates interatomic separations between adjacent Li sites of 2.64, 2.84, and 3.06 Å, with the shortest value corresponding to the edge-sharing LiO_4 tetrahedra. Hence, in contrast to the β_{II}-type structure of the cycled material, the

main Li migration paths in the as-prepared structure (γ_s) involve both edge- and corner-sharing LiO_4 tetrahedra with overall diffusion in the *b* direction and along the diagonal between the *a*- and *c*-axes.

Atomistic simulations were used to derive Li^+ migration energies for the paths shown in Figure 5. We also considered a range of other paths with longer Li—Li hop distances of >4.0 Å, but these all yielded very high migration barriers (>3.0 eV). The calculated Li^+ migration energies are listed in Table 3 and reveal two key points about the cycled structure. First, the lowest migration energy is 0.9 eV for the path in the *c* direction (hops A and B in Figure 5a), with a much higher barrier for the path along the *b*-axis. This suggests that Li transport involves zigzag paths between a corner-sharing network of Li1 and Li2 sites. The favorable Li^+ migration path involves passage through intervening vacant octahedral sites that share faces with the tetrahedral Li1 and Li2 sites. Recent DFT studies[15] based on earlier structural data[1,2a] have found Li-vacancy migration barriers of 0.9—1.0 eV in the delithiated system. It is interesting to note that the calculated migration energy is greater than the 0.6 eV reported for $LiFePO_4$.[8,16] Slower Li diffusion implies a lower rate capability for Li_2FeSiO_4 cathodes as Li is extracted and inserted over the composition range of the Li-rich solid solution.

In conclusion, the structure of cycled Li_2FeSiO_4 has been elucidated and the Li^+ migration pathways determined. The structure differs significantly from the as-prepared form and, as a consequence, so do the Li^+ diffusion pathways. In cycled Li_2FeSiO_4, all the Fe^{2+} and half the Li^+ share one set of tetrahedral sites (Li2/Fe) with the remaining Li^+ occupying a second set of tetrahedral sites (Li1). Li^+ transport in the cycled structure involves zigzag paths between corner-sharing Li1 and Li2 sites and through intervening vacant octahedral sites that share faces with the LiO_4 tetrahedra. The results presented here demonstrate that future work should consider how to synthesize the cycled structure directly, thus avoiding the structural changes on cycling, and how the structure may be modified to reduce the activation barrier for Li^+ diffusion, thus increasing the rate capability.

■ ASSOCIATED CONTENT

Supporting Information. Details of the refined structure of as-prepared Li_2FeSiO_4 and of the calculated structure. This material is available free of charge via the Internet at http://pubs.acs.org.

■ AUTHOR INFORMATION

Corresponding Author
p.g.bruce@st-and.ac.uk, m.s.islam@bath.ac.uk

■ ACKNOWLEDGMENT

The authors acknowledge the support of the EPSRC and the Supergen Energy Storage Consortium for funding, as well as Dr C. Eames (Bath) for useful discussions. The computations were run on the HECToR facilities via the Materials Chemistry Consortium. The authors are members of the Alistore-ERI.

■ REFERENCES

(1) (a) Nyten, A.; Abouimrane, A.; Armand, M.; Gustafsson, T.; Thomas, J. O. *Electrochem. Commun.* **2005**, *7*, 156. (b) Nyten, A.; Kamali, S.; Häggström, L.; Gustafsson, T.; Thomas, J. O. *J. Mater. Chem.* **2006**, *16*, 2266.

(2) (a) Dominko, R.; Bele, M.; Gaberscek, M.; Meden, A.; Remskar, M.; Jamnik, J. *Electrochem. Commun.* **2006**, *8*, 217. (b) Zaghib, K.; Ait Salah, A.; Ravet, N.; Mauger, A.; Gendron, F.; Julien, C. M. *J. Power Sources* **2006**, *160*, 1381. (c) Quoirin, G.; Taulelle, F.; Dupont, L.; Masquelier, C. *211th ECS Meeting*, 2007, Abstract #98. (d) Gong, Z. L.; Li, Y. X.; He, G. N.; Li, J.; Yang, Y. *Electrochem. Solid-State Lett.* **2008**, *11*, A60. (e) Zhang, S.; Deng, C.; Yang, S. Y. *Electrochem. Solid-State Lett.* **2009**, *12*, A136. (f) Boulineau, A.; Sirisopanaporn, C.; Dominko, R.; Armstrong, A. R.; Bruce, P. G.; Masquelier, C. *Dalton Trans.* **2010**, *39*, 6310. (g) Sirisopanaporn, C.; Boulineau, A.; Hanzel, D.; Dominko, R.; Budic, B.; Armstrong, A. R.; Bruce, P. G.; Masquelier, C. *Inorg. Chem.* **2010**, *49*, 7446. (h) Islam, M. S.; Dominko, R.; Masquelier, C.; Sirisopanaporn, C.; Armstrong, A. R.; Bruce, P. G. *J. Mater. Chem.* **2011**, *21*, 9811.

(3) (a) Gong, Z. L.; Li, Y. X.; Yang, Y. *Electrochem. Solid-State Lett.* **2006**, *9*, A542. (b) Kokalj, A.; Dominko, R.; Mali, G.; Meden, A.; Gaberscek, M.; Jamnik, J. *Chem. Mater.* **2007**, *19*, 3640. (c) Politaev, V. V.; Petrenko, A. A.; Nalbandyan, V. B.; Medvedev, B. S.; Shvetsova, E. S. *J. Solid State Chem.* **2007**, *180*, 1045. (d) Lyness, C.; Delobel, B.; Armstrong, A. R.; Bruce, P. G. *J. Chem. Soc., Chem. Commun.* **2007**, 4890. (e) Gong, Z. L.; Li, Y. X.; Yang, Y. *J. Power Sources* **2007**, *174*, 524. (f) Belharouak, I.; Abouimrane, A.; Amine, K. *J. Phys. Chem. C* **2009**, *113*, 20733.

(4) Nishimura, S.; Hayase, S.; Kanno, R.; Yashima, M.; Nakayama, N.; Yamada, A. *J. Am. Chem. Soc.* **2008**, *130*, 13212.

(5) Coelho, A. A. *J. Appl. Crystallogr.* **2000**, *33*, 899.

(6) (a) Catlow, C. R. A. *Computer Modeling in Inorganic Crystallography*; Academic Press: San Diego, CA, 1997. (b) Gale, J. D.; Rohl, A. L. *Mol. Simul.* **2003**, *29*, 291.

(7) (a) Kuganathan, N.; Islam, M. S. *Chem. Mater.* **2009**, *21*, 5196. (b) Islam, M. S. *Philos. Trans. R. Soc. A* **2010**, *368*, 3255.

(8) (a) Islam, M. S.; Driscoll, D. J.; Fisher, C. A. J.; Slater, P. R. *Chem. Mater.* **2005**, *17*, 5085. (b) Gardiner, G. R.; Islam, M. S. *Chem. Mater.* **2010**, *22*, 1242. (c) Fisher, C. A. J.; Hart Prieto, V. M.; Islam, M. S. *Chem. Mater.* **2008**, *20*, 5907.

(9) (a) Slater, B.; Catlow, C. R. A.; Liu, Z.; Ohsuna, T.; Terasaki, O.; Camblor, M. A. *Angew. Chem., Int. Ed.* **2002**, *41*, 1235. (b) Chiu, M. E.; Slater, B.; Gale, J. D. *Angew. Chem., Int. Ed.* **2005**, *44*, 1213. (c) Jones, A.; Islam, M. S.; Slater, P. R. *Chem. Mater.* **2008**, *20*, 5055.

(10) Eames C., Armstrong A. R., Bruce P. G., Islam M. S., in preparation

(11) Armstrong, A. R.; Lyness, C.; Ménétrier, M.; Bruce, P. G. *Chem. Mater.* **2010**, *22*, 1892.

(12) Liivat, A.; Larsson, P.; Thomas, J. O. Abstract 274, IMLB 2008, Tianjin, China, 2008.

(13) Wells, A. F. *Structural Inorganic Chemistry*; Clarendon Press: Oxford, 1984.

(14) Yamada, A.; Nishimura, S. Abstract O31, LiBD-4, Arcachon, France, 2009.

(15) Liivat, A.; Thomas, J. O. *Solid State Ionics* **2011**, *192*, 58.

(16) (a) Molenda, J.; Ojczyk, W.; Świerczek, K.; Zając, W.; Krok, F.; Dygas, J.; Liu, R. S. *Solid State Ionics* **2006**, *177*, 2617. (b) Amin, R.; Maier, J.; Balaya, P.; Chen, D. P.; Lin, C. T. *Solid State Ionics* **2008**, *179*, 1683.